International Journal of Pure and Applied Mathematics
Volume 59 No. 1 2010, 93-116

FUZZY TRACKING CONTROL FOR VEHICLES WITH SIDE SKIDDING

Keishi Shibayama[1], Valeri Kroumov[2 §], Akira Inoue[3]
Hirokazu Ohtagaki[4], Munaru Kawamura[5]

[1]Electric Power Development Co., Ltd.
6-15-1, Ginza, Chuo-ku, Tokyo, 104-8165, JAPAN
e-mail: keishi@scale-co.com

[2,4,5]Department of Electrical and Electronic Engineering
Okayama University of Science
1-1, Ridai-cho, Okayama, 700-0005, JAPAN
[2]e-mail: val@ee.ous.ac.jp
[4]e-mail: ohtagaki@ee.ous.ac.jp
[5]e-mail: minaru@ee.ous.ac.jp

[3]Graduate School of Natural Science and Technology
Okayama University
3-1-1, Tsushima-naka, Okayama, 700-8530, JAPAN
e-mail: inoue@suri.sys.okayama-u.ac.jp

Abstract: In this paper a novel fuzzy robust tracking controller for lateral vehicle guidance is proposed. A non-linear model of the vehicle is considered. The main feature of the proposed controller is that it consists of separate longitudinal (speed) and lateral (steer angle) controllers which, compared to single fuzzy controller designs, significantly reduces the complexity of the system. The controller assures robustness with respect to uncertainties in cornering forces and externally applied disturbances. The proposed controller can be applied to vehicles with understeer, oversteer and neutral steering behavior, and to vehicles which steering behavior change. Several simulation examples compare the proposed control scheme to some existing controllers and illustrate its effectiveness.

AMS Subject Classification: 93C42, 93C85, 70Q05
Key Words: fuzzy control, robust control, vehicle stability control, mobile

Received: January 12, 2010

§Correspondence author

robots, nonlinear syslems

1. Introduction

Fuzzy logic control proved to be an efficient way to realize effective control solutions in many engineering fields. Altrock and Krause [3] have been reported that many Japanese automotive companies make extensive use of fuzzy logic controllers to implement complex control strategies for various systems, such as anti-lock breaking system (ABS), anti spin regulator (ASR), engine control, etc. According to the research conducted by the Institute for Traffic Accident Research and Data Analysis (ITARDA) [18] in which three popular Toyota passenger cars, equipped with electronic stability control systems have been considered, 35% reduction in single car accidents, 30% reduction in head-on collision with other vehicles, and 35% reduction in casualties per year have been registered.

The methods for improving the lateral stability of vehicles include active steering control of front and/or rear tires as proposed by Hayama and Nishizaki [7], Nagai et al [14], Saito et al [16], Nonaka and Nakayama [15], and Hiraoka et al [8]; active suspension control (Gillespie [6]) of normal forces distribution at four wheels of the car and consequently affecting the tire lateral forces, and differential breaking control (Li et al [11], Shibahata et al [17]) which controls the tires longitudinal slip. Yet, because of the high cost, the implementation of the above three controllers together is rarely considered. On the other hand, the vehicle dynamics is very complex and has numerous uncertain, time-variant nonlinear characteristics. Therefore, it is very difficult to design a simple, highly reliable controller for such a complex system. In this paper we concentrate on the active steering control.

The vehicle steering control has been actively studied in the recent years and numerous approaches have been proposed. Due to the fact that vehicle model is nonlinear and in most cases possesses uncertainties, the classical linear control techniques are not directly applicable. There are two main types of control strategies for skidding vehicles: 1) sliding mode control as in Saito et al [16], Nonaka and Nakayama [15], Hiraoka et al [8], and 2) evolutionary methods, based mainly on fuzzy or/and neural control strategies, as proposed by von Altrock and Krause [3], Li et al [11], Lee et al [10].

In this paper we propose a robust fuzzy logic trajectory tracking controller for vehicles with front steering, subject to side skidding. It is assumed that

the model of the vehicle is unknown (see Kroumov et al [9]) and only knowledge available is that the tracking error is proportional to the control input. The proposed controller is successfully applied to linear and non-linear vehicle models and in both cases the control quality is very good. Additionally, a drive assist controller is developed. Compared to other control schemes for vehicle guidance, the controller design in proposed in this study is much simple. The design scheme is based on the Lyapunov stability theory which guarantees the overall stability of the system (Margaliot and Langholz [12]).

The rest of the paper is organized as follows: in the next section the non-linear and linear models of controlled four-wheel vehicle are presented. The lateral wind disturbance model is explained in the same section. Section 3 is devoted to design of the fuzzy controller. The proposed controller consists of separate longitudinal (speed) and lateral (steer angle) controllers. Using separate controllers instead of single fuzzy controller significantly reduces complexity of the system. Simulation results for linear and non-linear vehicle models are presented in Section 4. The simulations are performed for cornering on dry and wet roads with presence of side-wind disturbance. It is also shown that the proposed control scheme performs very well for over steered and under steered cars. In the last section some conclusions and plans for further developments are presented.

2. Problem Formulation

2.1. 2 DOF Vehicle Model

Generally, the dynamic behavior of a vehicle is determined by the forces imposed on it from the tires, gravity, and aerodynamics. The vehicle is studied to determine what forces will be produced by each of these sources at particular maneuver and how the vehicle will respond to these forces.

In this study, a 2 DOF nonlinear vehicle model is adopted, that is a forward and yaw dynamics. The model is depicted in Figure 1. Figures 2 and 3 show the forces acting on the tires of the vehicle. When the vehicle moves with velocity v, the forward and lateral forces acting on the body are expressed as (Gillespie [6])

$$\begin{aligned} Ma_x &= F_{X_{fr}}\cos\delta_r - F_{Y_{fr}}\sin\delta_r + F_{X_{fl}}\cos\delta_l - F_{Y_{fl}}\sin\delta_l \\ &\quad + F_{X_{rr}} + F_{X_{rl}} + F_{x_d}, \end{aligned} \tag{1}$$

$$Ma_y = F_{X_{fr}}\sin\delta_r + F_{Y_{fr}}\cos\delta_r + F_{X_{fl}}\sin\delta_l + F_{Y_{fl}}\cos\delta_l \tag{2}$$

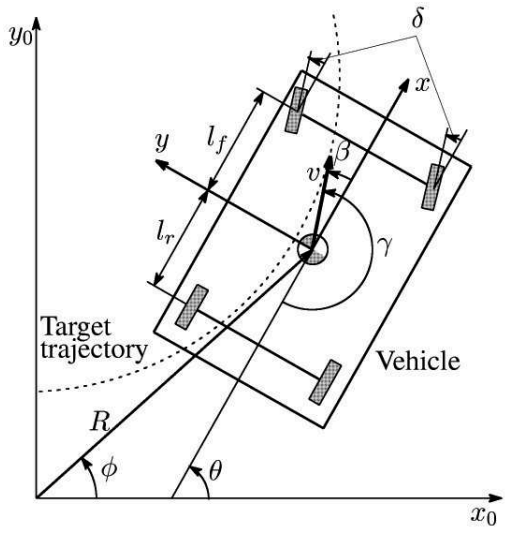

Figure 1: 2 DOF vehicle model

$$
\begin{aligned}
& +F_{Y_{rr}} + F_{Y_{rl}} + F_{y_d} \\
I\dot{\gamma} \;=\; & l_f(F_{X_{fr}} \sin\delta_r + F_{Y_{fr}} \cos\delta_r) + \frac{d_f}{2}(F_{X_{fr}} \cos\delta_r - F_{Y_{fr}} \sin\delta_r) \qquad (3) \\
& + l_f(F_{X_{fl}} \sin\delta_l + F_{Y_{fl}} \cos\delta_l) - \frac{d_f}{2}(F_{X_{fl}} \cos\delta_l - F_{Y_{fl}} \sin\delta_l) \\
& - l_r(F_{Y_{rr}} + F_{Y_{rl}}) + \frac{d_r}{2}(F_{X_{rr}} - F_{X_{rl}}) + N_d.
\end{aligned}
$$

The vehicle acceleration components along x and y axes are

$$
\begin{aligned}
a_x &= -v(\dot{\beta} + \gamma)\sin\beta + \dot{v}\cos\beta, \qquad (4) \\
a_y &= v(\dot{\beta} + \gamma)\cos\beta + \dot{v}\sin\beta.
\end{aligned}
$$

Further, substituting the right sides of (2) and (3) by f_x and f_y respectively gives the following nonlinear vehicle model:

$$
\dot{v} = \frac{1}{M}(f_x \cos\beta + f_y \sin\beta), \qquad (5)
$$

$$
\dot{\beta} = \frac{1}{Mv}(f_x \sin\beta + f_y \cos\beta) - \gamma, \qquad (6)
$$

$$
\begin{aligned}
\dot{\gamma} \;=\; & \frac{l_f}{I}(F_{X_{fr}} \sin\delta_r + F_{Y_{fr}} \cos\delta_r) + \frac{d_f}{2I}(F_{X_{fr}} \cos\delta_r - F_{Y_{fr}} \sin\delta_r) \qquad (7) \\
& + \frac{l_f}{I}(F_{X_{fl}} \sin\delta_l + F_{Y_{fl}} \cos\delta_l) - \frac{d_f}{2I}(F_{X_{fl}} \cos\delta_l - F_{Y_{fl}} \sin\delta_l)
\end{aligned}
$$

$$-\frac{l_r}{I}(F_{Y_{rr}} + F_{Y_{rl}}) + \frac{d_r}{2I}(F_{X_{rr}} - F_{X_{rl}}) + \frac{N_d}{I},$$

where M is the mass of the body, β is the slip angle, γ is the yaw rate, I is the vehicle yaw moment of inertia, and F_f, F_r are the cornering forces acting at front and rear wheels, respectively. The rest of the symbols used throughout the text are as follows:

l_f, l_r	distances between the centre of gravity (CG) and front and rear wheels, respectively;
C_f, C_r	cornering stiffness at front and rear wheels;
ϕ	heading angle;
$(x_0,\ y_0)$	fixed (world) coordinate system;
$(x,\ y)$	vehicle coordinate system;
$(X,\ Y)$	tire coordinate system;
d_f, d_r	tread;
$F_{X_{fr}}$, $F_{X_{fl}}$	front tires forces in X direction;
$F_{X_{rr}}$, $F_{X_{rl}}$	rear tires forces in X direction;
$F_{Y_{fr}}$, $F_{Y_{fl}}$	front tires forces in Y direction;
$F_{Y_{rr}}$, $F_{Y_{rl}}$	rear tires forces in Y direction;
F_{x_d}, F_{y_d}	disturbance along x and y axes;
N_d	moment of inertia caused by the disturbance;
v	the body velocity;
θ	yaw angle;
δ_r, δ_l	the left and right tire angles.

2.2. Tire Dynamics

2.2.1. Nonlinear Tire Model

Because it is easy to handle, in many up-to-date results, the linearized model of the cornering power have been used. In this paper we are using a non-linear presentation of the cornering power in order to derive more realistic model of the vehicle dynamics as suggested by Ali and Sjöberg [2].

The cornering power depends on many variables: tire size and type, number of pliers, cord angles, wheel width and tread are most significant. The "magic formula", proposed by Bakker et al [4], is one of often used models of the forces that are generated by the tire, but because it needs a lot of experimental data to build a proper model of a *concrete* tire, in this study we are using the Fiala's

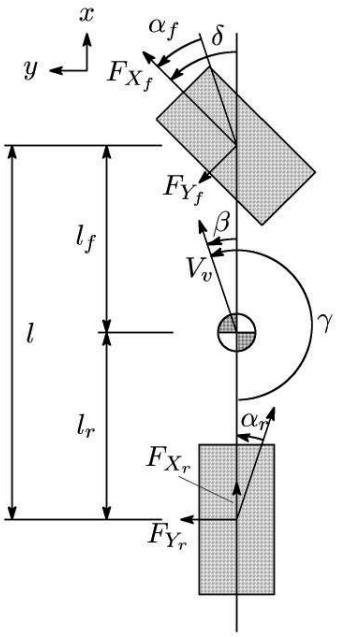

Figure 2: Distributions of the forces, acting on front and rear tires

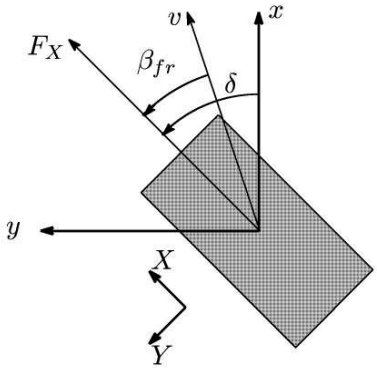

Figure 3: Tire model

model [5]:

$$F_Y(\beta_{fr}) = \frac{C_1 l^2}{2}\tan\beta_{fr} - \frac{1}{8}\frac{C_1^2 l^3}{\mu p b}\tan^2\beta_{fr} \qquad (8)$$

$$+\frac{1}{96}\frac{C_1^3 l^4}{\mu^2 p^2 b^2}\tan^3\beta_{fr},$$

$$C_1 = \frac{C_0}{1+\frac{\left(4\sqrt{\frac{4}{EJ}}\right)^3 l^3 C_0}{12k}}, \tag{9}$$

$$C_0 = \frac{b}{T}G, \tag{10}$$

where μ is a static friction coefficient, p is the maximum inflation pressure, T is the tread, b is the tread contact width, l is the tread contact length, k is elasticity coefficient, E is the material elasticity coefficient at the tread base, J is the moment of inertia at the tread radius, G is the cornering stiffness, and C_0 is the longitudinal creep stiffness. The above equation is for the model of front right tire and respective equations are used for the rest of the tires.

The slip angles of the front and rear tires are

$$\beta_{fr} = \arctan\left(\frac{v\sin\beta + l_f\gamma}{v\cos\beta + \gamma\frac{d_f}{2}}\right) - \delta, \tag{11}$$

$$\beta_{fl} = \arctan\left(\frac{v\sin\beta + l_f\gamma}{v\cos\beta - \gamma\frac{d_f}{2}}\right) - \delta,$$

$$\beta_{rr} = \arctan\left(\frac{v\sin\beta - l_r\gamma}{v\cos\beta + \gamma\frac{d_r}{2}}\right), \tag{12}$$

$$\beta_{rl} = \arctan\left(\frac{v\sin\beta - l_r\gamma}{v\cos\beta - \gamma\frac{d_r}{2}}\right).$$

Figures 2 and 3 depict the forces acting on a vehicle tire.

2.2.2. Linear Tire Model

For the sake of comparison, the linearized model of a tire is presented here.

The cornering forces $F_{Y_{fr}}$, $F_{Y_{fl}}$, $F_{Y_{rr}}$, $F_{Y_{rl}}$ grow with the slip angle β. At low slip angles (less than 5 degrees) the relation is linear and the cornering force can be described by (Gillespie [6])

$$F_Y = C\beta, \tag{13}$$

where C is known as the cornering stiffness.

Setting $\beta \ll 1$ and $d/(2v) \ll 1$ in (11) gives:

$$\begin{aligned} F_{Y_{fr}} &= -C_f \left(\beta + \frac{l_f \gamma}{v} - \delta_r \right), \\ F_{Y_{fl}} &= -C_f \left(\beta + \frac{l_f \gamma}{v} - \delta_l \right), \\ F_{Y_{rr}} &= F_{Y_{rl}} = -C_r \left(\beta - \frac{l_r \gamma}{v} \right). \end{aligned} \tag{14}$$

2.3. Linearized Vehicle Model

Supposing that the tire angles, the body slip angle β, and the yaw rate γ are sufficiently small the linearised vehicle body model can be derived from (2), (3), (4), and (14).

$$\begin{aligned} mv(\dot{\beta} + \gamma) &= 2f_f + 2f_r + F_{y_d}, \\ I\dot{\gamma} &= (2l_f f_f - 2l_r f_r - l_F F_{y_d})\beta. \end{aligned} \tag{15}$$

By defining a state vector $\boldsymbol{x}^T = [\beta \;\; \gamma]$ the state equations become:

$$\begin{aligned} \dot{\boldsymbol{x}} &= \boldsymbol{A}\boldsymbol{x} + \boldsymbol{B}\boldsymbol{u} + \boldsymbol{h}F_{y_d}, \\ \boldsymbol{u}^T &= \begin{bmatrix} \delta_r & \delta_l \end{bmatrix}, \\ \boldsymbol{A} &= \begin{bmatrix} \frac{-2(C_f + C_r)}{Mv} & \frac{-2(C_f l_f - C_r l_r)}{Mv^2} - 1 \\ \frac{-2(C_f l_f + C_r l_r)}{I} & \frac{-2(C_f l_f^2 + C_r l_r^2)}{Iv} \end{bmatrix}, \\ \boldsymbol{B} &= \begin{bmatrix} \frac{C_f}{Mv} & \frac{C_f}{Mv} \\ \frac{C_f l_f}{I} & \frac{C_f l_f}{I} \end{bmatrix}, \quad \boldsymbol{h} = \begin{bmatrix} \frac{1}{Mv} & \frac{-l_F}{I} \end{bmatrix}, \end{aligned} \tag{16}$$

where l_F is the distance from the CG to the point the disturbance is acting on.

2.4. Wind Disturbance Model

For lateral guidance only the lateral disturbance F_{y_d} and the lateral yaw moment N_d are of importance ($F_{x_d} = 0$). The forces from lateral wind are expressed according to Milliken and Milliken [13]:

$$F_{y_d} = W_y \rho S \frac{(v\cos\beta)^2 + (v\sin\beta + w)^2}{2}, \tag{17}$$

$$N_d = W_n \rho S (l_f + l_r) \frac{(v\cos\beta)^2 + (v\sin\beta + w)^2}{2}, \tag{18}$$

where, S is the area of the vehicle that is exposed to the wind, ρ is the mass density of the air, w is the wind speed, W_y, W_n are lateral and yawing aerodynamic drag coefficients, and are given by

$$\begin{aligned} W_y &= C_y \beta_w, \\ W_n &= C_n \beta_w, \\ \beta_w &= \arctan \frac{v \sin \beta + w}{v \cos \beta}. \end{aligned} \tag{19}$$

3. Fuzzy Controller Design

The proposed fuzzy controller is shown in Figure 4. The longitudinal (speed) and lateral (steer angle) controllers are separate. Using separate controllers instead of single fuzzy controller significantly reduces complexity of the system. Further, it is assumed that the model of the vehicle is unknown and the only knowledge available about the system is that the tracking error is proportional to the control input. Both controllers are of PID type.

3.1. Fuzzy Lateral Controller

The control should minimize the error e between the desirable trajectory R_r and the vehicle's actual trajectory R, i.e.

$$e(t) = R_r - R \to 0. \tag{20}$$

Let us define a Lyapunov function as follows

$$V(e) = \frac{1}{2} \left[\left(\int_0^t e(\tau)\, d\tau \right)^2 + e^2 + \dot{e}^2 \right]. \tag{21}$$

The system is asymptotically stable if the following conditions hold:

$$V(0) = 0, \tag{22}$$

$$V(\infty) = \infty, \tag{23}$$

$$\dot{V}(e) = e \int_0^t e(\tau)\, d\tau + e\dot{e} + \dot{e}\ddot{e} < 0. \tag{24}$$

Assuming that $\ddot{e}$ is proportional to the control input δ, (24) can be rewritten as (see Appendix B):

$$\dot{V}(e) \approx e \int_0^t e(\tau)\, d\tau + e\dot{e} + \dot{e}\delta < 0. \tag{25}$$

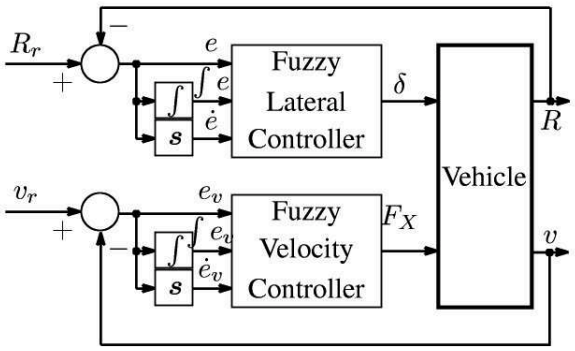

Figure 4: Block diagram of the controller

Now, let every variable in (25) is characterized by a pair of positive e_{j_+} and a negative e_{j_-} $(j = p, i, d)$ fuzzy number. Substituting these values in (25) gives the following set of conditions satisfying (25):

$$\begin{aligned}
e_{p_+}e_{i_+} + e_{p_+}e_{d_+} + e_{d_+}\delta < 0, \\
e_{p_+}e_{i_+} + e_{p_+}e_{d_-} + e_{d_-}\delta < 0, \\
e_{p_-}e_{i_+} + e_{p_-}e_{d_+} + e_{d_+}\delta < 0, \\
e_{p_-}e_{i_+} + e_{p_-}e_{d_-} + e_{d_-}\delta < 0, \\
e_{p_+}e_{i_-} + e_{p_+}e_{d_+} + e_{d_+}\delta < 0, \\
e_{p_+}e_{i_-} + e_{p_+}e_{d_-} + e_{d_-}\delta < 0, \\
e_{p_-}e_{i_-} + e_{p_-}e_{d_+} + e_{d_+}\delta < 0, \\
e_{p_-}e_{i_-} + e_{p_-}e_{d_-} + e_{d_-}\delta < 0,
\end{aligned} \tag{26}$$

which can be expressed directly as fuzzy rules:

$$\begin{aligned}
&\text{IF } e_{p_+} \text{ AND } e_{d_+} \text{ AND } e_{i_+} \quad \text{THEN} \quad \delta \text{ IS } \delta_{1_-} \\
&\text{IF } e_{p_+} \text{ AND } e_{d_-} \text{ AND } e_{i_+} \quad \text{THEN} \quad \delta \text{ IS } \delta_{3_+} \\
&\text{IF } e_{p_-} \text{ AND } e_{d_+} \text{ AND } e_{i_+} \quad \text{THEN} \quad \delta \text{ IS } \delta_0 \\
&\text{IF } e_{p_-} \text{ AND } e_{d_-} \text{ AND } e_{i_+} \quad \text{THEN} \quad \delta \text{ IS } \delta_{2_+} \\
&\text{IF } e_{p_+} \text{ AND } e_{d_+} \text{ AND } e_{i_-} \quad \text{THEN} \quad \delta \text{ IS } \delta_{2_-} \\
&\text{IF } e_{p_+} \text{ AND } e_{d_-} \text{ AND } e_{i_-} \quad \text{THEN} \quad \delta \text{ IS } \delta_0 \\
&\text{IF } e_{p_-} \text{ AND } e_{d_+} \text{ AND } e_{i_-} \quad \text{THEN} \quad \delta \text{ IS } \delta_{3_-} \\
&\text{IF } e_{p_-} \text{ AND } e_{d_-} \text{ AND } e_{i_-} \quad \text{THEN} \quad \delta \text{ IS } \delta_{1_+}
\end{aligned} \tag{27}$$

We choose for the linguistic terms in the IF parts the following membership

functions:

$$\begin{aligned} e_{p_+} &= e^{-q_1(x-k_1)^2}, \quad e_{p_-} = e^{-q_1(x+k_1)^2}, \\ e_{i_+} &= e^{-q_2(x-k_2)^2}, \quad e_{i_-} = e^{-q_2(x+k_2)^2}, \\ e_{d_+} &= e^{-q_3(x-k_3)^2}, \quad e_{d_-} = e^{-q_3(x+k_3)^2}, \end{aligned} \tag{28}$$

(29)

where q_1, q_2, q_3, k_1, k_2, and k_3 are positive constants and x is for e, $\dot{e}$ and $\int e(\tau)\,d\tau$. The linguistic terms in the THEN parts are given by:

$$\begin{aligned} \delta_{1_+} &= e^{-(\delta-c_1)^2}, \quad \delta_{1_-} = e^{-(\delta+c_1)^2}, \\ \delta_{2_+} &= e^{-(\delta-c_2)^2}, \quad \delta_{2_-} = e^{-(\delta+c_2)^2}, \\ \delta_{3_+} &= e^{-(\delta-c_3)^2}, \quad \delta_{3_-} = e^{-(\delta+c_3)^2}, \\ \delta_0 &= e^{-\delta^2}. \end{aligned} \tag{30}$$

The control input δ is implemented as a centre of gravity defuzzifier:

$$\delta = \frac{\int \mu(z)\mu(\delta)\,dz}{\int \mu(z)\,dz}. \tag{31}$$

Theorem 1. *Let the membership functions for the fuzzy rules (27) are given as in (28) and (30). Then the fuzzy controller (31) is stable.*

Proof. The proof is given in Appendix. □

3.2. Fuzzy Velocity Controller

The velocity fuzzy controller is implemented almost as the tracking controller. Substituting δ with F_X and e with $e_v = v_r(t) - v(t)$ (v_r: desired velocity, v: measured velocity) in (21)–(30) gives the velocity controller realization (see Figure 4.).

3.3. Fuzzy Driver Assist Controller

The developed fuzzy driver-assist controller is depicted in Figure 5. The driver-assist controller generates a compensating signal δ_c in order to adjust the tire angle δ of the vehicle. This makes the vehicle to exactly follow the model behavior. Here δ_r is the reference tire angle which is applied only to the vehicle model.

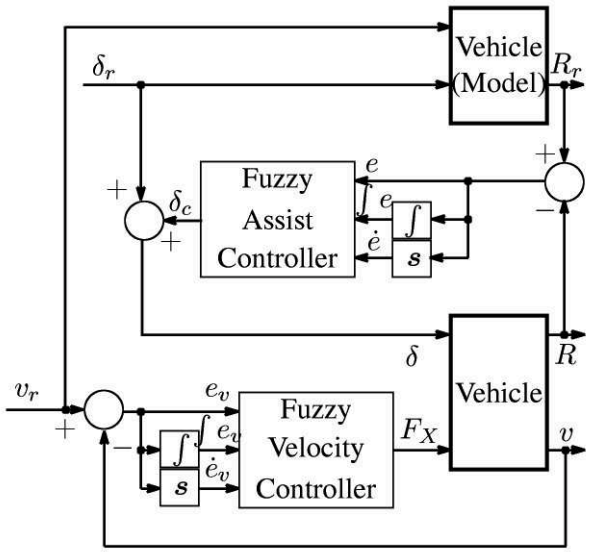

Figure 5: Block diagram of the assist controller

4. Simulation Results

Several simulations were run to investigate the performance of the proposed control scheme. For these simulations the linear and non-linear models as described in Sections 2.1 and 2.2 were used. The vehicle parameters are the same as in Nonaka and Nakayama [15] and are depicted in Table 1. The parameters of the fuzzy controllers are given in Table 2. The values of c_1, c_2 and c_3 are chosen to keep e (e_v), $\int e(t)\,dt$ ($\int e_v(t)\,dt$) and $\dot{e}$ ($\dot{e}_v$) inside the allowable boundaries. The transient properties of the tire angles δ and tire forces F_x depend on k_1, k_2 and k_3. The coefficients q_1, q_2 and q_3 are for adjusting the PID controller parameters.

The tire model parameters are shown in Table 3. The cornering force from Nonaka and Nakayama [15] were used to calculate the parameters of the model of the tire. With the values of these parameters when the friction constant μ is set to 1.0 the tires lateral forces become equal to the contact ground pressure.

The reference trajectory is described as $R_r(\phi) = 15 + 10\cos(\phi/2)$ $(-4\pi < \phi \leq 4\pi)$, the initial car position was set to $\boldsymbol{R}^T = [0,\ 26,\ \pi/2]$, and the initial velocity $v(0)$ is 1 m/s for all simulations.

Parameter	Value
M	1717kg
I	2741.9kg·m^2
l_f	1.01m
l_r	1.68m
d_f	1.5m
d_r	1.5m
C_f	34455N/rad
C_r	25703N/rad

Table 1: Vehicle parameters

	Controller	
Variable	Lateral	Velocity
k_1	2.0	6000
k_2	1.5	3000
k_3	0.02	200
q_1	7.0	0.3
q_2	5.0	0.03
q_3	0.02	0.02
c_1	0.5	2.5
c_2	1.5	18
c_3	2.0	5.0

Table 2: Fuzzy controller parameters

4.1. Linear Model

This simulation was performed only to make a comparison with the results of Nonaka and Nakayama [15]. Figure 6 depicts the simulation result for tracking control when the linear model of the vehicle is used. The velocity was set 7.5 m/s. The trajectory error and the steering angle are shown in Figure 7 and Figure 8, respectively.

The tracking error at steady state is between -0.088 m and 0.022 m. At time t=30 s, C_f and C_r were reversed, which changes the vehicle behavior from over steer to under steer (Gillespie [6]) and as it may be confirmed from the above figures that this change does not affect the system behavior.

Parameter	Value(Front Tire)	Value(Rear Tire)
C_1	27564000	27564000
l	0.1 [m]	0.1 [m]
p	130600 [N]	78500 [N]
b	0.6 [m]	0.6 [m]

Table 3: Tire model parameters (Fiala model)

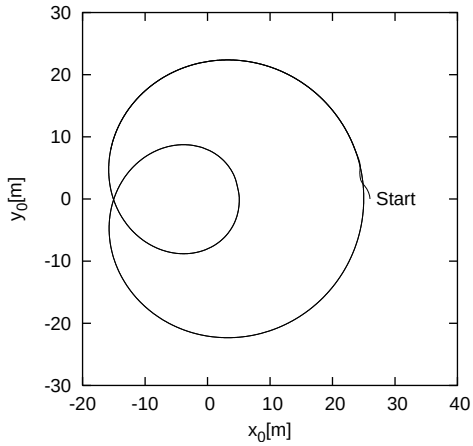

Figure 6: Trajectory of vehicle (oversteer and understeer linear model)

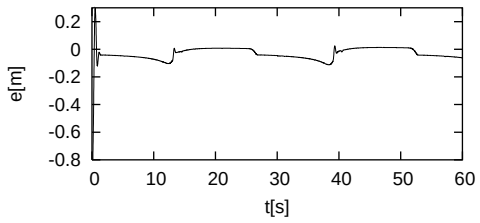

Figure 7: Trajectory error (oversteer and understeer linear model)

4.2. Nonlinear Model

For the nonlinear model of the vehicle, the simulations were performed using the following parameters: forces from the body acting on front and rear axes 5224

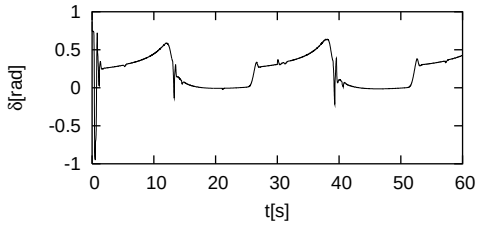

Figure 8: Tire steering angle (oversteer and understeer linear model)

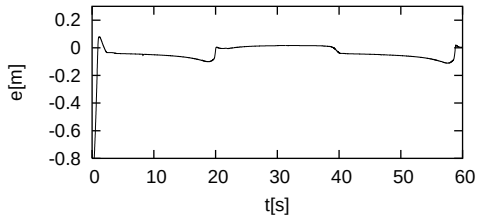

Figure 9: Trajectory error (nonlinear model, dry ($\mu = 0.9$) road and wet ($\mu = 0.4$) road)

N, and 3140 N, respectively, and the parameters tire model (Fiala's model) (8) are as shown in Table 3. The trajectories of the vehicle in the following simulations are not shown for brevity – visually they do not differ from Figure 6.

4.2.1. Wet Road

Figures 9 and 10 show the simulation results for wet road. The initial conditions and the reference trajectory are identical to the conditions in Section 4.1. The dry road friction coefficient ($\mu = 0.9$) was changed at $t = 30$ s to wet road friction, i.e. $\mu = 0.4$.

The maximum tracking steady state error for dry road is in the range -0.073 m–0.013 m and for wet road on the range -0.076 m–0.013 m.

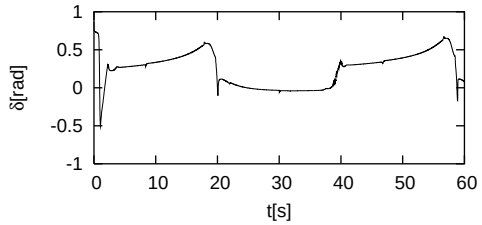

Figure 10: Steering angle (nonlinear model, dry ($\mu = 0.9$) road and wet ($\mu = 0.4$) road)

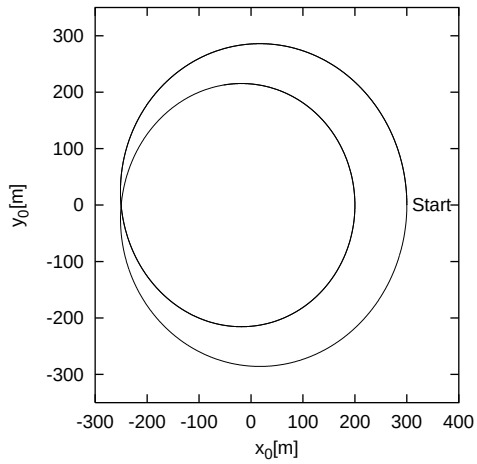

Figure 11: Trajectory of vehicle (dry road and wind $w = 35$ m/s)

4.2.2. Lateral Wind Disturbance

The parameters for the wind model (17) were chosen as $\rho = 1.245$ kg/m^3, $S = 1.92$ m^2, $W_Y = 1.576$, and $W_N = 0.6446$. For these simulations the vehicle speed was increased to approximately 60 km/h. In order to simulate a realistic drive run, the trajectory was adjusted according to the road regulations (minimum curve radius of 220 m) as shown in Figure 11. The simulation results are shown in Figure 12–14. The simulation was performed for dry road condition ($\mu = 0.9$), and the wind velocity was set to $w = 35$ m/s. The wind was applied

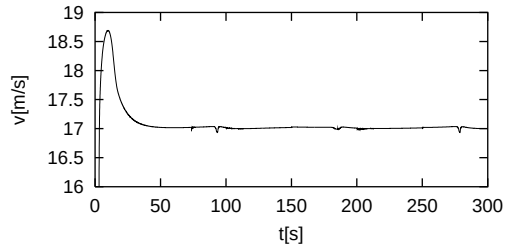

Figure 12: Car velocity (dry road and wind $w = 35$ m/s)

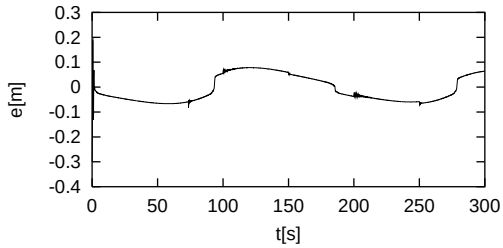

Figure 13: Trajectory error (dry road and wind w=35 m/s)

for 50 s at time $t = 100$ s and $t = 200$ s. The initial speed of the car was set to 5 m/s. In Figure 12 after acceleration for 3.3 s, the speed reaches the steady state value at $t = 15.9$ and clearly the effect of the lateral wind disturbance is suppressed very well.

The tracking error (see Figure 13) varies between -0.082 m and 0.079 m. It can be seen from Figure 14 and Figure 15 that at the extreme situation at $t = 100$ s, because of the strong wind, the steering angle and the lateral angle of the vehicle are in opposite each other directions. This means that the vehicle follows the trajectory while skidding. In real situations, when a vehicle start to skid, the driver decreases the speed to bring the car out of the skid, but in the simulations here the controller runs the car with a constant, actually, quite dangerous velocity. It can be concluded that the trajectory tracking controller performs very well, but in the future research a machanism, which does not allow the car to go into skid have to be developed.

A comparison to a patented PID controller [1] is given in Appendix C.

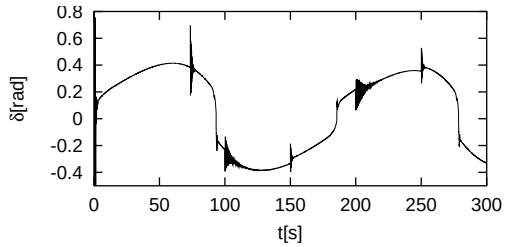

Figure 14: Tire steering angle (dry road and wind w=35m/s)

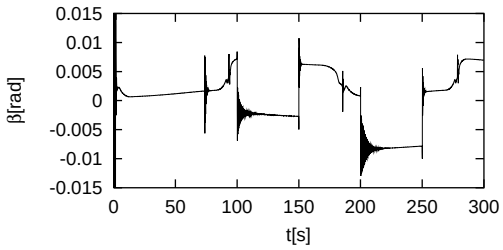

Figure 15: Lateral angle (dry road and wind $w = 35$ m/s)

4.2.3. Driver Assist Control

The simulation result for the drive assist control is shown in Figure 16 and Figure 17. The reference steering angle was set as $\delta_r = 0.15(1 - \cos(1.115t))$ in order to make R_r to represent a clothoid curve. For a reference model of the car the linearized model from Section 2.3 was used. The model has a neutral steering behavior with $l_f = l_r = 1.245$ m and cornering force of 30079. The simulation results show that the tracking error varies between -0.0084 m and 0.0037 m. Adding a lateral wind with velocity of 15 m/s slightly affects the error: the eror was between -0.0074m and 0.0097m.

It may be concluded that the simulation results well prove that the proposed fuzzy controller performs very well.

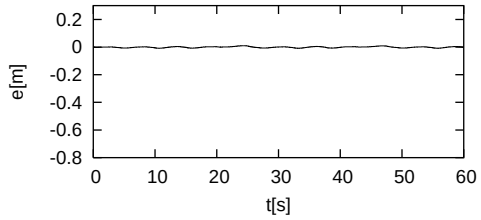

Figure 16: Assist error (nonlinear model, dry road and wind $w = 15$ m/s)

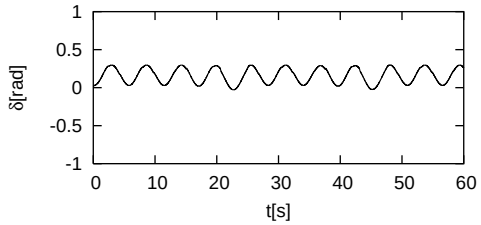

Figure 17: Assisted steering angle (nonlinear model, dry road and wind $w = 15$ m/s)

5. Discussion and Conclusions

In this paper a fuzzy robust tracking controller for lateral vehicle guidance have been proposed. The controller consists of separate longitudinal (speed) and lateral (steer angle) controllers which significantly reduces complexity of the system, compared to single fuzzy controller designs. It was assumed that the model of the vehicle is unknown and only knowledge available is that the tracking error is proportional to the control input. The methodology for choosing and adjusting the fuzzy rules is very simple and effective and can be employed for fuzzy controller designs in other fields. It assures robustness with respect to uncertainties in cornering forces and externally applied disturbances like wet road and lateral wind. The simulation examples show that the proposed scheme is very effective.

The following developments are in progress: 1) Redesign of controller for known vehicle model, i.e. Takagi-Sugeno type of controller. This will allow to better realize a model following control scheme and we expect that such design will give better tracking results. Moreover, changing the type of the model steering, such controller may allow to change the steering behavior of

the controlled vehicle. For instance, applying an over steered model to an under steered car would lead to over steered car behavior and vise verse; 2) adding of a driver's model and a model of the steering wheel system; 3) design of controller for 4WS model; and 4) development of a controller for individually breaking the car wheels. These will allow realizing more realistic and applicable control system. A hardware implementation of the proposed controller is also planned.

References

[1] T. Akita, Drive Assist Device, Pat. No. 2006-236238, Japanese Patent Office, Japan (2006).

[2] M. Ali, J. Sjöberg, Impact of Different Vehicle Models on Threat Assessment in Critical Curve Situations, 21st International Technical Conference on the Enhanced Safety of Vehicles (ESV), available: http://www-nrd.nhtsa.dot.gov/departments/esv/21st/ (2009).

[3] C. von Altrock, B. Krause, Fuzzy logic and neurofuzzy technologies in embedded automotive applications, In: *Third International Conference on Industrial Fuzzy Control and Intelligent Systems (IFIS '93)*, Houston, Texas, USA (1993), 55-59.

[4] E. Bakker, L. Nyborg, H. B. Pajeika, Tire modelling for use in vehicle dynamics studies, *SAE Tech. Pap. Ser.*, No. 870495 (1987).

[5] E. Fiala, Lateral forces on rolling pneumatic tires, *Zeitschrift, V.D.I.*, **96**, No. 29 (1954), 973-979.

[6] T.D. Gillespie, *Fundamentals of Vehicle Dynamics*, Warrendale, PA: Society of Automotive Engineers, Inc. (1992), 195-236.

[7] R. Hayama, K. Nishizaki, The vehicle stability control responsibility improvement using steer by wire, In: *Proc. of the IEEE Intelligent Vehicle Symposium*, Dearbom (MI), USA (2000).

[8] T. Hiraoka, O. Nishihara, H. Kumamoto: Path tracking of four wheel steering vehicle by using sliding mode control, *Trans. of the Institute of Systems, Control and Information Engineers*, **16**, No. 10 (2003), 520-530.

[9] V. Kroumov, K. Shibayama, H. Ohtagaki, Fuzzy tracking control for lateral vehicle guidance, In: *Proc. IASTED Int. Conf. on Modelling, Identification, and Control (MIC 2007)*, Innsbruck, Austria (2007), 234-240.

[10] G. D. Lee, S.W. Kim, T.J. Park, Premise-part adaptation laws for adaptive fuzzy control and its applications to vehicle speed control, In: *Proc. 40-th IEEE Conf. on Decision and Control*, Orlando (FL), USA (2001), 2460-2465.

[11] Y.D. Li, W. Liu, J. Li, Z.M. Ma, J.C. Zhang, Simulation of vehicle stability control system using fuzzy PI control method, In: *IEEE Int. Conf. on Vehicular Electronics and Safety*, Xi'an, China (2005), 165-170.

[12] M. Margaliot, G. Langholz, *New Approaches to Fuzzy Modeling and Control – Design and Analysis*, World Scientific Publishing Co. Pte. Ltd., Singapore (2000).

[13] W.F. Milliken, D.L. Milliken, *Race Car Vehicle Dynamics*, Warendale: SAE international (1995).

[14] M. Nagai, M. Shino, F. Gao, Study of integrated control of active front steer angle and direct yaw moment, *JSAE Review*, **23** (2002), 309-315.

[15] K. Nonaka, H. Nakayama, Robust tracking control based on exact linearization for vehicles with side skidding, *Trans. of the Society of Instrument and Control Engineers*, **42**, No. 6 (2006), 603-610.

[16] S. Saito, K. Nonaka, D.N. Nenchev, H. Katayama, Sliding mode control of a skidding car: A quantitative analysis through interactive driving, In: *Proc. of SICE Annual Conference (SICE2004)*, Sapporo, Japan (2004), 2251-2254.

[17] Y. Shibahata, K. Shimada, T. Tomari, Improvement of vehicle manoeuvrability by direct yaw moment control, *Vehicle System Dynamics*, **22** (1993), 465-481.

[18] Available: http://www.nhtsa.gov/portal/site/nhtsa/template.MAXIMIZE/menuitem.081e9 2a06f83bfd24ec86e10dba046a0/ (2009).

Appendix A: Proof of Theorem 1

Proof. In the following proof for the sake of simplicity, the fuzzy positive and negative values will be presented using (*pos*) and (*neg*). Also for δ_{3_-}, δ_{2_-}, δ_{1_-}, δ_{1_+}, δ_{2_+}, δ_{3_+}, δ_0 we are going to use (*neg_big*), (*neg_med*), (*neg_small*), (*pos_small*), (*pos_med*), (*pos_big*), and (*zero*), respectively.

For some $k_1 > 0$ and $k_2 > 0$ we can rewrite (24) as

$$\dot{V} = k_1 e \int_0^t e(\tau)\, d\tau + k_2 e\dot{e} + \dot{e}\delta.$$

Using this, the first rule in (27) can be rewritten as

$$\dot{V} \approx (pos)(pos)(pos) + (pos)(pos)(pos) + (pos)(neg\_big) \tag{32}$$

which directly gives a fuzzy rule about $\dot{V}$

$$\begin{aligned} &\text{IF} \quad e > 0 \quad \text{AND} \quad \int_0^t e(\tau)d\tau > 0 \quad \text{AND} \quad \dot{e} > 0 \\ &\quad \text{THEN} \quad (pos)(pos)(pos) + (pos)(pos)(pos) + (pos)(neg\_big). \end{aligned} \tag{33}$$

In the same way, the rest of the rules from (27) give

$$\begin{aligned} &\text{IF} \quad e > 0 \quad \text{AND} \quad \int_0^t e(\tau)d\tau > 0 \quad \text{AND} \quad \dot{e} < 0 \\ &\quad \text{THEN} \quad (pos)(pos)(pos) + (pos)(pos)(neg) + (neg)(pos\_small) \end{aligned} \tag{34}$$

$$\begin{aligned} &\text{IF} \quad e > 0 \quad \text{AND} \quad \int_0^t e(\tau)d\tau < 0 \quad \text{AND} \quad \dot{e} > 0 \\ &\quad \text{THEN} \quad (pos)(pos)(neg) + (pos)(pos)(pos) + (pos)(neg\_med) \end{aligned}$$

$$\begin{aligned} &\text{IF} \quad e > 0 \quad \text{AND} \quad \int_0^t e(\tau)d\tau < 0 \quad \text{AND} \quad \dot{e} < 0 \\ &\quad \text{THEN} \quad (pos)(pos)(neg) + (pos)(pos)(neg) \end{aligned}$$

$$\begin{aligned} &\text{IF} \quad e < 0 \quad \text{AND} \quad \int_0^t e(\tau)d\tau > 0 \quad \text{AND} \quad \dot{e} > 0 \\ &\quad \text{THEN} \quad (pos)(neg)(pos) + (pos)(neg)(pos) \end{aligned}$$

$$\begin{aligned} &\text{IF} \quad e < 0 \quad \text{AND} \quad \int_0^t e(\tau)d\tau > 0 \quad \text{AND} \quad \dot{e} < 0 \\ &\quad \text{THEN} \quad (pos)(neg)(pos) + (pos)(neg)(neg) + (neg)(pos\_med) \end{aligned}$$

$$\begin{aligned} &\text{IF} \quad e < 0 \quad \text{AND} \quad \int_0^t e(\tau)d\tau < 0 \quad \text{AND} \quad \dot{e} > 0 \\ &\quad \text{THEN} \quad (pos)(neg)(neg) + (pos)(neg)(pos) + (pos)(neg\_small) \end{aligned}$$

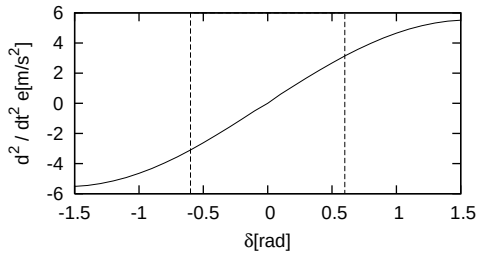

Figure 18: Steering angle δ vs. lateral error acceleration $\ddot{e}$ (parameters from Section 4)

$$\text{IF} \quad e < 0 \quad \text{AND} \quad \int_0^t e(\tau)d\tau < 0 \quad \text{AND} \quad \dot{e} < 0$$
$$\text{THEN} \quad (pos)(neg)(neg) + (pos)(neg)(neg) + (neg)(pos\_big)$$

If k_1 and k_2 are properly chosen, $\dot{V}$ can become negative, from which the system stability directly follows. □

Appendix B: About the Proportionality between the Steering Angle and the Error Acceleration

The fuzzy controller designed in Section 3 is based on the assumption that the acceleration of the position error $\ddot{e}$ depends linearly on the steering angle δ. To show this it is possible to derive a function describing this dependency from the model presented in Sections 2.1, 2.2, 2.4, and from $\ddot{e} = \frac{d^2}{dt^2}(R_r - R)$. Because such a function will be very complicated the linear dependence would not be straightforward, a simulation result showing the proportionality between $\ddot{e}$ and δ is shown here. In the simulation result depicted in Figure 18 the change of the steering angle for a real vehicle is between the dashed lines. It is obvious that within this interval both parameters are approximately linearly proportional each other.

Appendix C: Comparison to a Classical PID Control

A simulation to compare the proposed in this paper controller to the PID control from Japanese patent No. 2006-236238 [1] is shown in Figure 19. The tracking error of the patented controller is very large: it varies between -0.8 m and 0.3

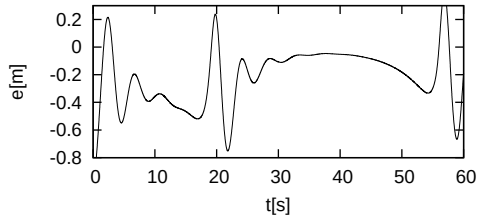

Figure 19: Trajectory error (dry ($\mu = 0.9, t < 30$) road and wet ($\mu = 0.4, t \geq 30$) road)

m. Clearly, such an error may become a cause of accident. It is obvious that the proposed here controller is superior to the patented one.